RSC Advances

PAPER

View Article Online
View Journal | View Issue

Cite this: *RSC Adv.*, 2017, **7**, 18851

Investigation of the dinuclear effect of aluminum complexes in the ring-opening polymerization of ε-caprolactone†

Chiao-Yin Hsu,[a] Hsi-Ching Tseng,[a] Jaya Kishore Vandavasi,[c] Wei-Yi Lu,[a] Li-Fang Wang,[a] Michael Y. Chiang,[ab] Yi-Chun Lai,[a] Hsing-Yin Chen*[a] and Hsuan-Ying Chen *[ad]

A series of aluminum (Al) complexes bearing hydrazine-bridging Schiff base and salen ligands were synthesized and investigated as catalysts for the ring-opening polymerization of ε-caprolactone (CL). The introduction of steric bulky groups increases the catalytic activity of the corresponding mononuclear aluminum complex. However, the opposite phenomenon was observed in dinuclear Al complexes bearing salen ligands because the steric repulsion reduced the cooperative activation mechanism in the dinuclear Al system. Among these Al complexes, L^{N2Bu}-Al_2Me_4 bearing a hydrazine-bridging Schiff base ligand had the highest catalytic activity, approximately 3- to 11-fold higher than that of dinuclear Al complexes bearing salen ligands and mononuclear Al complexes bearing Schiff base ligands. Density functional theory calculations revealed that the mechanism of the coordination of CL to one Al center was initiated by the benzyl alkoxide of another Al center.

Received 21st February 2017
Accepted 22nd March 2017

DOI: 10.1039/c7ra02136d

rsc.li/rsc-advances

1. Introduction

Biodegradable polymers such as poly-ε-caprolactone (PCL) were designed not only to resolve the pollution problem caused by petrochemical plastics, but also as biomaterials for various fields such as tissue engineering,[1a–c] bone regeneration,[1d] drug carriers,[1e] and biomedical application[1f–i] because of its biodegradability, biocompatibility, and permeability. The use metal complexes[2] as catalysts for the ring-opening polymerization (ROP) of ε-caprolactone (CL) leads to efficient synthesis of PCL, and aluminum complexes[3,4] are common catalysts for ROP because of their ease of synthesis, the low cost of their precursor materials, and the highly catalytic conversion rate of their CL polymerization. The catalytic activity of aluminum (Al) complexes in cycloester ROP may be improved by ligand modification because the influences of ligands including steric, electronic, and chelating effects, directly change the catalytic activity of metal complexes.[3f] Recently, dinuclear Al catalysts[5,6] were used in cycloesters ROP, and some ROPs,[6] shown in Fig. 1, proved that dinuclear Al complexes have higher catalytic activity than do mononuclear Al complexes.

A possible coordination–insertion mechanism[6a] (Fig. 2) was reported, in which one Al atom serves as the Lewis acid to activate the monomer by the monomer coordination. An alkoxy group on the second Al atom initiates the carbonyl group of the monomer, and monomer ring opens into another alkoxy group. The polymer chain alternates between two Al atoms, making it an extremely efficient polymerization process. Carpentier[6e] reported that the Al–Al distance in his study is 2.8–3.0 Å, which could open up a cooperatively activation mechanism.

Dinuclear Ti complexes[7] bearing hydrazine-bridging Schiff base ligands shown in Fig. 3, have been used as catalysts in L-lactide polymerization, where they had higher catalytic activity than did mononuclear Ti complexes bearing Schiff base ligands. The Ti–Ti distance in that study was 3.244 Å with two bridging isopropoxides. Hydrazine-bridging Schiff base ligands appear to be the perfect ligands for use in a dinuclear Al system in CL polymerization. Herein, a series of hydrazine-bridging Schiff base ligands, salen ligands, Schiff base ligands, and associated Al complexes were synthesized. The catalytic comparison in CL polymerization between di- and mononuclear Al complexes and the possible mechanism using density functional theory (DFT) were studied.

2. Results and discussion

2.1. Synthesis and characterization of Al complexes

Symmetrical and asymmetrical hydrazine-bridging Schiff base ligands,[7] and salen ligands[8] were synthesized using acid-

[a]Department of Medicinal and Applied Chemistry, Kaohsiung Medical University, Kaohsiung 80708, Taiwan, Republic of China. E-mail: hchen@kmu.edu.tw; Fax: +886-7-3125339; Tel: +886-7-3121101-2585

[b]Department of Chemistry, National Sun Yat-Sen University, Kaohsiung 804, Taiwan, Republic of China

[c]Department of Chemistry, University of Ottawa, Ontario, Canada

[d]Department of Medical Research, Kaohsiung Medical University Hospital, Kaohsiung 80708, Taiwan, Republic of China

† Electronic supplementary information (ESI) available: Polymer characterization data, and details of the kinetic study. CCDC 1482938. For ESI and crystallographic data in CIF or other electronic format see DOI: 10.1039/c7ra02136d

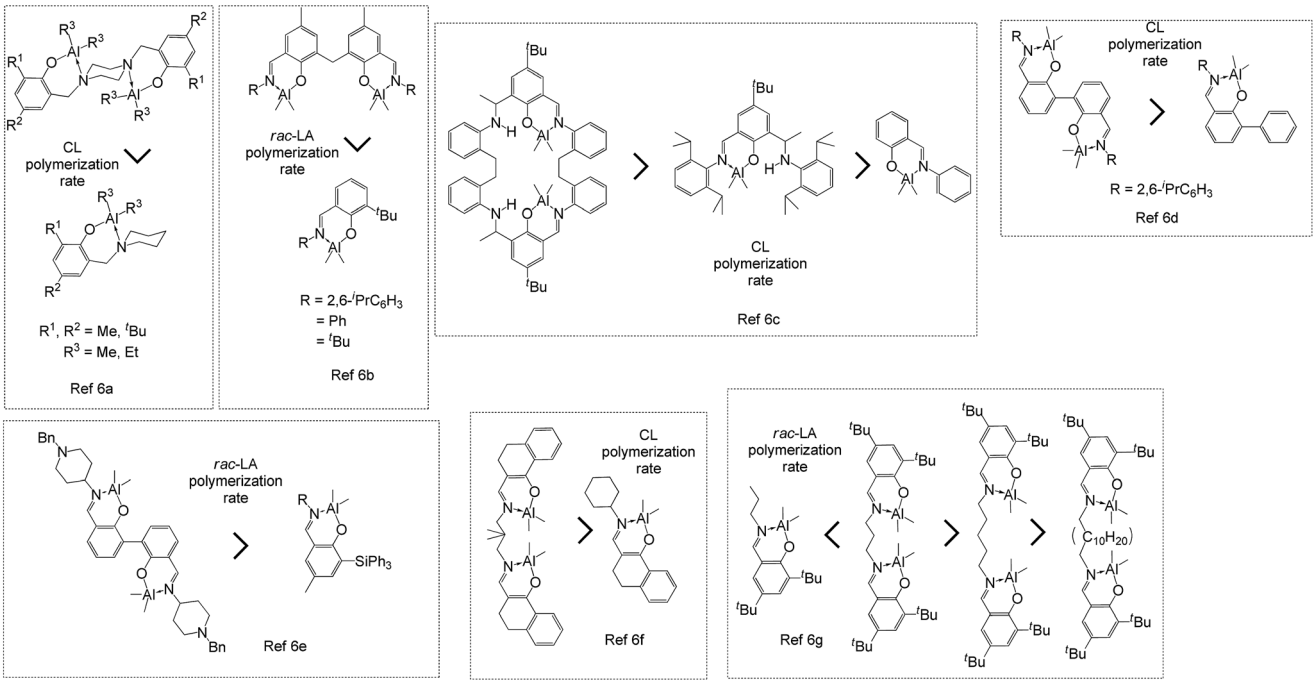

Fig. 1 Structures and their catalytic activity of Al complexes bearing Schiff base ligands.

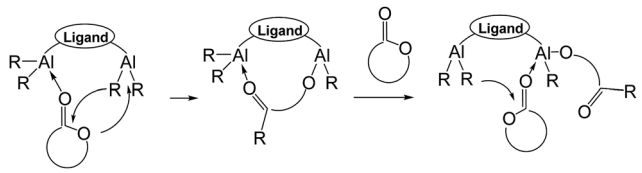

Fig. 2 Possible coordination–insertion mechanism of cyclic ester ROP by using dinuclear Al complexes as catalysts.

catalyzed condensation following the literature procedures. The synthesis of Al complexes was described in Experimental section, and Al complexes were obtained as evidenced by the appearance of methyl groups showed a singlet peak in the upfield region (−0.5 to −0.75 ppm) and an 6 : 1 integral ratio (two methyl groups : one imine proton) in ^{1}H NMR spectra. The crystal of $\mathbf{L^{ClBu}}$-$\mathbf{AlMe_2}$ (**5**) was observed in $CDCl_3$ in the nuclear magnetic resonance (NMR) tube at −20 °C after 1 month.

The X-ray structure of $\mathbf{L^{ClBu}}$-$\mathbf{AlMe_2}$ (**5**) (Fig. 4, CCDC 1482938) illustrates the distorted tetrahedral geometry of the Al complex with two methyl groups. The angles of the N(1)–Al(1)–O(1) and C(23)–Al(1)–C(24) planes are 93.32(6)° and 119.59(8)°, respectively. The distances of Al(1)–O(1), Al(1)–N(1), Al(1)–C(23), and Al(1)–C(24) are 1.7624(12), 1.9923(15), 1.9563(19), and 1.9587(19) Å, respectively.

2.2. Polymerization of ε-caprolactone

CL polymerization in toluene using Al complexes as catalysts with BnOH as the initiator was investigated in a nitrogen atmosphere at room temperature (Table 1 and Fig. 5). As shown in entries 1–8 of Table 1, all Al complexes were active in CL polymerization, and dinuclear Al complexes, $\mathbf{L^{N-NH}}$-$\mathbf{Al_2Me_4}$ (**2**) and $\mathbf{L^{N-NBu}}$-$\mathbf{Al_2Me_4}$ (**3**), and mononuclear Al complex, $\mathbf{L^{ClH}}$-$\mathbf{AlMe_2}$ (**2**), exhibited a low controllability of larger M_{nGPC} and a broad polydispersity index (PDI, 1.70–2.18) compared with

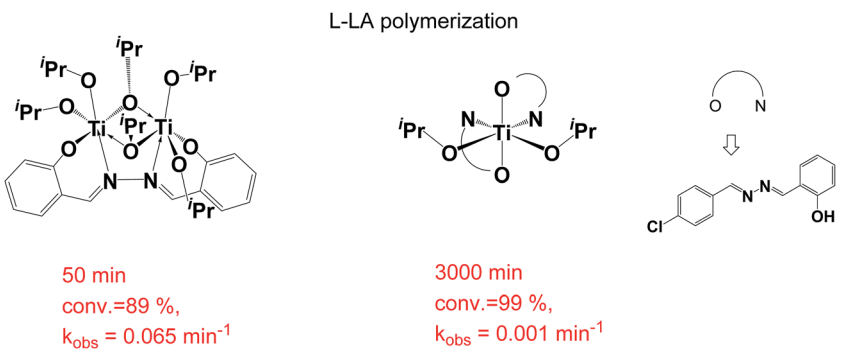

Fig. 3 Comparison of L-LA polymerization between di- and mononuclear Ti complexes.

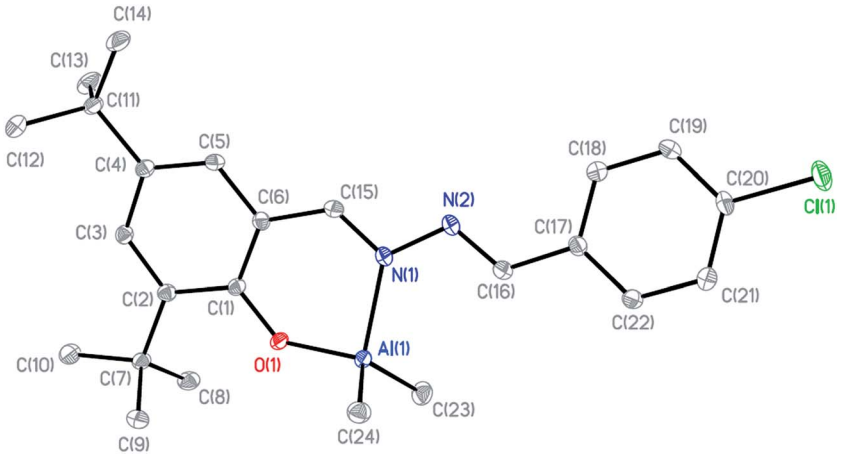

Fig. 4 Molecular structure of L^{ClBu}-$AlMe_2$ (5) as 30% probability ellipsoids (all of the hydrogen atoms were omitted for clarity).

other Al complexes, and it may be ascribed to the trans-esterification[9e] or produce inactive impurity after the reaction of BnOH and Al complexes. In dinuclear Al complexes, the catalytic activity of $\mathbf{L^{N2Bu}\text{-}Al_2Me_4}$ (**1**) bearing a hydrazine-bridging Schiff base ligand was higher (approximately 3- to 11-fold) than that of Al complexes bearing salen and Schiff base ligands. This reveals that the dinuclear Al complex bearing a hydrazine-bridging Schiff base ligand has greater cooperation than those bearing salen ligands. $\mathbf{L^{N-NBu}\text{-}Al_2Me_4}$ (**1**) exhibited a lower polymerization rate than did $\mathbf{L^{N-NH}\text{-}Al_2Me_4}$ (**2**), revealing that a steric bulky ligand decreased the catalytic activity of Al complexes. However, in mononuclear Al complexes, the opposite phenomenon was observed, similar to in the literature.[4f] This may be because the cooperation between the two Al centers was blocked by the steric bulky ligand in the dinuclear system. In addition, mononuclear Al complexes bearing hydrazine-bridging Schiff base ligands, $\mathbf{L^{ClH}\text{-}AlMe_2}$ (**4**) and $\mathbf{L^{ClBu}\text{-}AlMe_2}$ (**5**), revealed the greater catalytic activity than those, $\mathbf{L^{HBu}\text{-}AlMe_2}$ (**6**), $\mathbf{L^{Bu}\text{-}AlMe_2}$ (**7**), and $\mathbf{L^{Bn}\text{-}AlMe_2}$ (**8**), bearing normal Schiff base ligands. This may be attributed to hydrazine group, as an electron withdrawing group, increasing the Lewis acidity of the Al center. On the basis of the linear relationship between M_{nGPC} and ($[CL]_0$ × conv.)/[BnOH] exhibited in Fig. 6, polymerizing CL by using $\mathbf{L^{N2Bu}\text{-}Al_2Me_4}$ (**1**) as the catalyst demonstrated high controllability with a narrow PDI.

The ^{1}H NMR spectrum of PCL (Fig. 7, PCL from entry 11, Table 1) shows that peaks at 7.36 ppm ($C_6H_5CH_2$–, peak a), 5.12 ppm ($C_6H_5CH_2$–, peak b), and 3.66 ppm (CH_2CH_2OH, peak c) with an integral ratio of 5 : 2 : 2 between H_a, H_b, and $H_{c'}$,

Table 1 ε-Caprolactone polymerization by using each of the Al complexes as catalysts at room temperature[d]

Entry	Catalyst	Time (min)	Conv.[a] (%)	M_{nCal}[b]	M_{nGPC}[c]	M_{nNMR}[b]	PDI[c]	k_{obs} (error)/min
1[d]	$\mathbf{L^{N2Bu}\text{-}Al_2Me_4}$ (**1**)	60/90	80/88	5100	7200	5900	1.20	0.0261 (22)
2[d]	$\mathbf{L^{N-NH}\text{-}Al_2Me_4}$ (**2**)	60/1395	46/95	5500	11 800	11 200	2.18	0.0085 (4)
3[d]	$\mathbf{L^{N-NBu}\text{-}Al_2Me_4}$ (**3**)	60/1330	9/100	5800	11 600	5800	1.70	0.0023 (8)
4[e]	$\mathbf{L^{ClH}\text{-}AlMe_2}$ (**4**)	60/720	22/99	5800	16 100	11 000	1.73	0.0065 (7)
5[e]	$\mathbf{L^{ClBu}\text{-}AlMe_2}$ (**5**)	60/230	28/95	5500	5000	3700	1.16	0.0098 (4)
6[e]	$\mathbf{L^{HBu}\text{-}AlMe_2}$ (**6**)[4r]	60/1260	18/94	5500	5900	6700	1.15	0.0021 (1)
7[e]	$\mathbf{L^{Bu}\text{-}AlMe_2}$ (**7**)	60/360	17/90	5300	6900	6900	1.16	0.0065 (3)
8[e]	$\mathbf{L^{Bn}\text{-}AlMe_2}$ (**8**)	60/2560	0/96	5600	7700	4200	1.16	0.0014 (5)
9[f]	$\mathbf{L^{N2Bu}\text{-}Al_2Me_4}$ (**1**)	1000	96	11 100	29 700	11 500	1.39	0.0035 (2)
10[g]	$\mathbf{L^{N2Bu}\text{-}Al_2Me_4}$ (**1**)	30	97	2900	3100	4700	1.06	0.1413 (72)
11[h]	$\mathbf{L^{N2Bu}\text{-}Al_2Me_4}$ (**1**)	20	99	1500	1600	2300	1.06	0.2541 (127)
12[i]	$\mathbf{L^{N2Bu}\text{-}Al_2Me_4}$ (**1**)	450	90	11 500	22 300	11 500	1.31	—[l]
13[j]	$\mathbf{L^{N2Bu}\text{-}Al_2Me_4}$ (**1**)	1500	95	16 400	47 400	17 100	1.30	—[l]
14[k]	$\mathbf{L^{N2Bu}\text{-}Al_2Me_4}$ (**1**)	1500	96	22 000	57 400	20 300	1.32	—[l]

[a] Obtained from ^{1}H NMR analysis. [b] Calculated from the molecular weight of monomer × $[monomer]_0/[BnOH]_0$ × conversion yield + M_w(BnOH). [c] Obtained from GPC analysis and calibration based on the polystyrene standard. Values of M_{nGPC} are the values obtained from GPC times 0.56. [d] Reaction condition: toluene (5 mL), [CL] = 2.0 M, [CL] : [Cat] : [BnOH] = 100 : 0.5 : 2. [e] Reaction condition: toluene (5 mL), [CL] = 2.0 M, [CL] : [Cat] : [BnOH] = 100 : 1 : 2. [f] Reaction condition: toluene (5 mL), [CL] = 2.0 M, [CL] : [Cat] : [BnOH] = 100 : 0.25 : 1.0. [g] Reaction condition: toluene (5 mL), [CL] = 2.0 M, [CL] : [Cat] : [BnOH] = 100 : 1 : 4. [h] Reaction condition: toluene (5 mL), [CL] = 2.0 M, [CL] : [Cat] : [BnOH] = 100 : 2 : 8. [i] Reaction condition: toluene (5 mL), [CL] = 4.0 M, [CL] : [Cat] : [BnOH] = 200 : 0.5 : 2. [j] Reaction condition: toluene (5 mL), [CL] = 6.0 M, [CL] : [Cat] : [BnOH] = 300 : 0.5 : 2. [k] Reaction condition: toluene (5 mL), [CL] = 8.0 M, [CL] : [Cat] : [BnOH] = 400 : 0.5 : 2. [l] Not available.

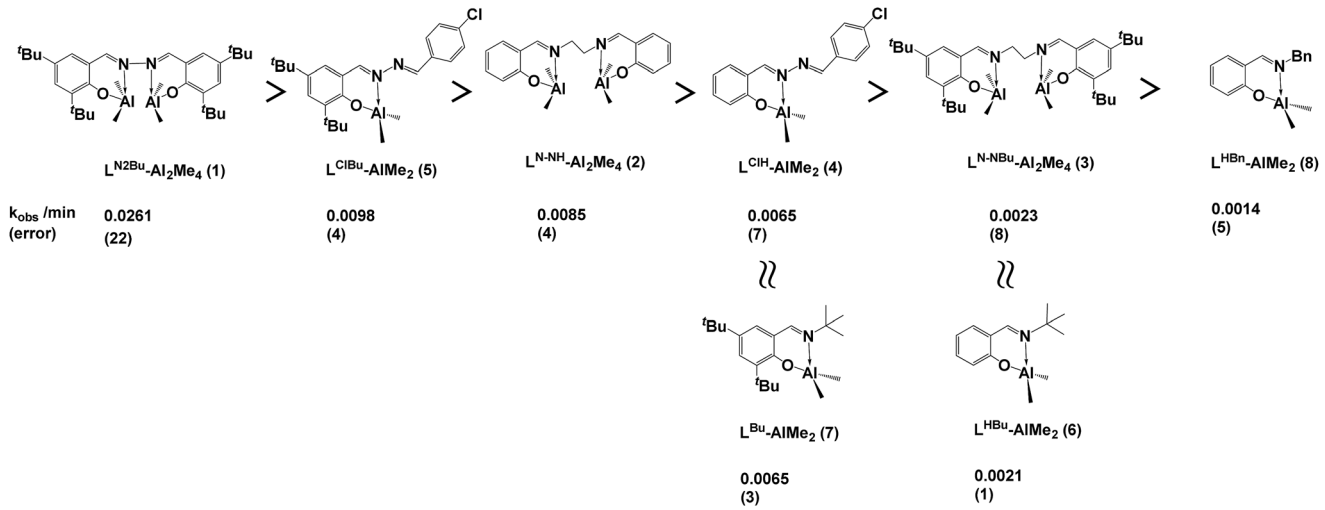

Fig. 5 Comparison of the catalytic activity of di- and mononuclear Al complexes.

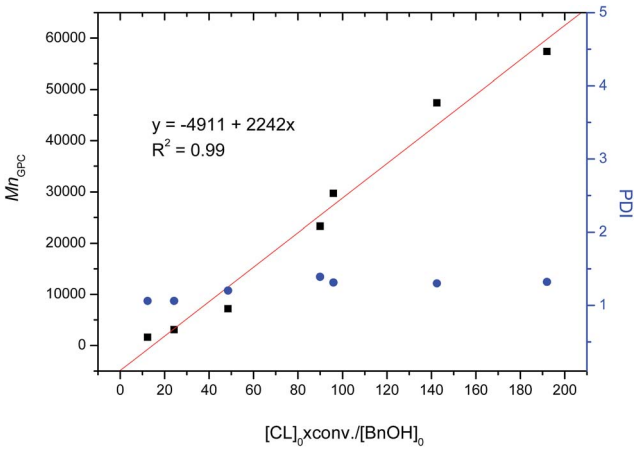

Fig. 6 Linear plot of M_{nGPC} *versus* $[CL]_0 \times$ conv./$[BnOH]_0$ with blue dots indicating polydispersity indices (Table 1, entries 1 and 9–14).

indicating that the polymer chain should be capped with one benzyl ester and one hydroxy end and suggesting that the polymerization occurs through the insertion of a benzyl alkoxy group into CL.

2.3. Kinetic studies of CL polymerization catalyzed by L^{N2Bu}-Al_2Me_4

Kinetic studies were performed at room temperature with respect to the ratio of $[CL]_0/[\mathbf{L^{N2Bu}\text{-}Al_2Me_4}\ (\mathbf{1}) + 4BnOH]$ ($[CL] =$ 2.0 M in 5 mL of toluene) as shown in Table S2 and Fig. S2.† The preliminary results indicated a first-order dependency on [CL] (Fig. S2†). By plotting k_{obs} against $[\mathbf{L^{N2Bu}\text{-}Al_2Me_4}\ (\mathbf{1}) + 4BnOH]$, a k_{prop} values of 7.37 (M^{-1} min^{-1}) was obtained (Fig. 8). Polymerizing CL by using $\mathbf{L^{N2Bu}\text{-}Al_2Me_4}$ (**1**) at room temperature demonstrated the following rate law:

$$d[CL]/dt = 7.37 \times [CL][\mathbf{L^{N2Bu}\text{-}Al_2Me_4}\ (\mathbf{1}) + 4BnOH]$$

2.4. Polymerization mechanism of L^{N2Bu}-Al_2Me_4 using DFT calculation

To shed some light on how dinuclear Al catalysts cooperatively polymerizate the CL, DFT calculations were performed for the $\mathbf{L^{N2Bu}\text{-}Al_2Me_4}$ (**1**) system. To reduce the computational cost, the ^{t}Bu groups on the hydrazine-bridging Schiff base ligand were replaced by hydrogen atoms and the methoxide was used instead of benzyl alkoxide.

The structure of the active catalyst from the reaction of $\mathbf{L^{N2Bu}\text{-}Al_2Me_4}$ (**1**) with 4 equivalent of BnOH could not be isolated in the experiments. However, the ^{1}H NMR spectrum (Fig. S17†) of the mixture of benzyl alcohol and $\mathbf{L^{N2Bu}\text{-}Al_2Me_4}$ (**1**) revealed that methyl groups associated with Al center disappear, and new methylene groups of benzyl alkoxide grow up. Based on the acceptable assumption that alcohol is able to replace methyl groups[3b–e,j–n,4q,r] and referring to the crystal structure of dinuclear Ti catalyst previously reported,[7] our DFT calculations successfully located the optimized geometry of the dinuclear Al catalyst (Fig. 9). In this C2 symmetric structure, two Al metals are bridged by two alkoxide groups with an Al–Al distance of 2.83 Å. The coordination geometry of the Al metals is characterized by a distorted square pyramid in which four oxygen atoms form the base and a nitrogen atom is located at the apex. The vacant site opposite to the nitrogen can be used to accommodate the CL monomer.

The DFT-calculated reaction pathway and the related free energy changes for the ROP of CL by the dinuclear Al catalyst are illustrated in Fig. 10. The first step is the association of CL and the catalyst. The calculations predict that CL can coordinate with the Al center through the carbonyl oxygen ($O_{carbonyl}$) to form a stable complex **a**, which is 2.6 kcal mol^{-1} lower than the separated state. We also considered the Al–CL complex bound through the ester oxygen (O_{ester}) of CL; nonetheless, the binding free energy of the O_{ester}-bound complex is 1.1 kcal mol^{-1}, indicating that it is not a stable complex. That CL prefers coordination to the Al center *via* $O_{carbonyl}$ rather than O_{ester} has been reported previously.[4s]

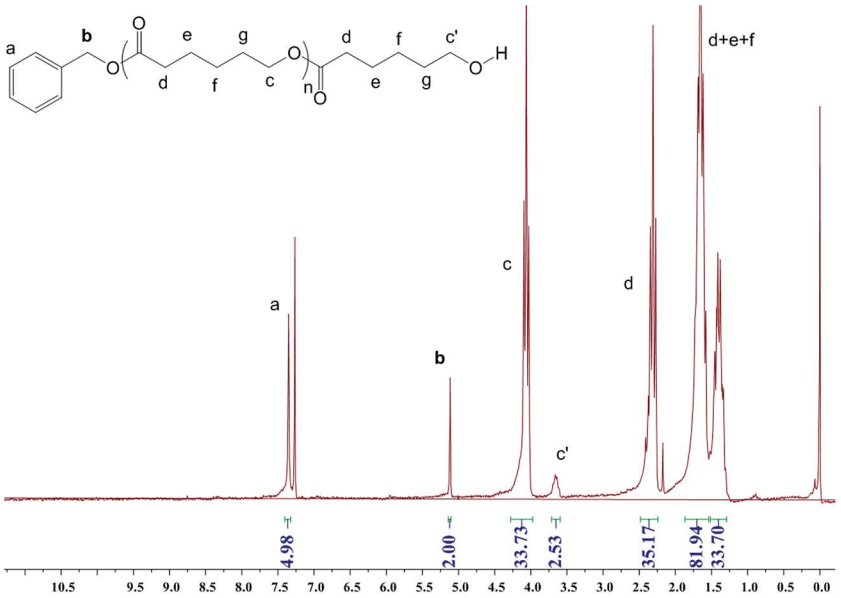

Fig. 7 ^{1}H NMR spectrum of PCL in $CDCl_3$ catalyzed by L^{N2Bu}-Al_2Me_4 (**1**) with BnOH (entry 11, Table 1).

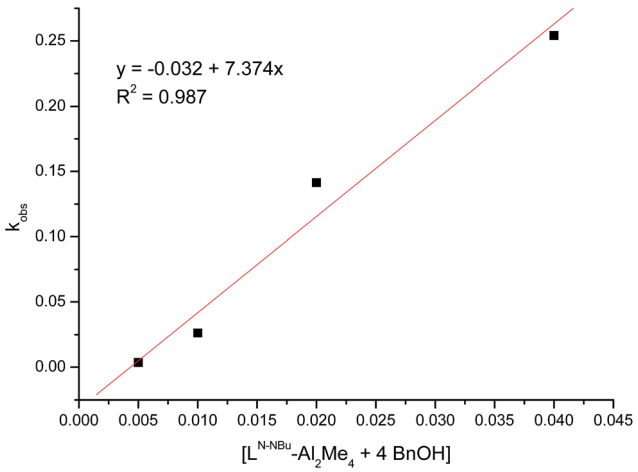

Fig. 8 Linear plot of k_{obs} against [L^{N2Bu}-Al_2Me_4 (**1**) + 4BnOH] for CL polymerization with [CL] = 2.0 M in toluene (5 mL).

Upon association with the CL monomer, one of the bridging alkoxides leaves the CL-coordinated Al center (**a** → **b**) and then inserts into the activated carbonyl carbon (**b** → **c**). Notice that during the alkoxide insertion, the ester oxygen of CL concurrently coordinates to the other Al center but the ring structure of CL remains closed. The CL in **c** immediately undergoes ring opening to achieve a more thermodynamically more stable state **d**. It is assumed that the free CL monomers could subsequently attack the $O_{carbonyl}$-coordinated Al center (right Al site) of **d** and dissociate the carbonyl group of the open-ring CL to generate a new propagating alkoxide; that is, return to state **b** to accomplish the catalytic cycle. According to the present DFT calculations, the rate of propagation is determined by the step of alkoxide insertion **b** → **c** with an activation free energy of 19.2 kcal mol^{-1}. This theoretical value is in good agreement with the experimental measurement of the propagating rate constant k_{prop} = 7.37 M^{-1} min^{-1}, which equates to an activation free energy of 18.7 kcal mol^{-1} using the Eyring equation.

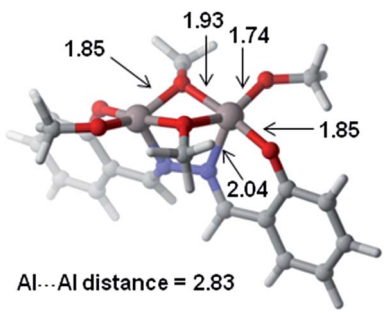

Fig. 9 DFT-optimized structure of an active dinuclear Al catalyst (distances in angstroms).

3. Conclusions

A comparison of CL polymerization between mononuclear Al complexes bearing Schiff base ligands, and dinuclear Al complexes bearing hydrazine-bridging Schiff base and salen ligands was investigated. Mononuclear Al complexes with steric bulky groups increased the catalytic activity, whereas the opposite phenomenon was observed in dinuclear Al complexes bearing salen ligands. Steric repulsion may reduce the cooperatively activation mechanism in a dinuclear Al system. L^{N2Bu}-Al_2Me_4 (**1**) bearing a hydrazine-bridging Schiff base ligand had the highest catalytic activity (approximately 3- to 11-fold), higher than that of dinuclear Al complexes bearing salen ligands and mononuclear Al complexes bearing Schiff base ligands. A

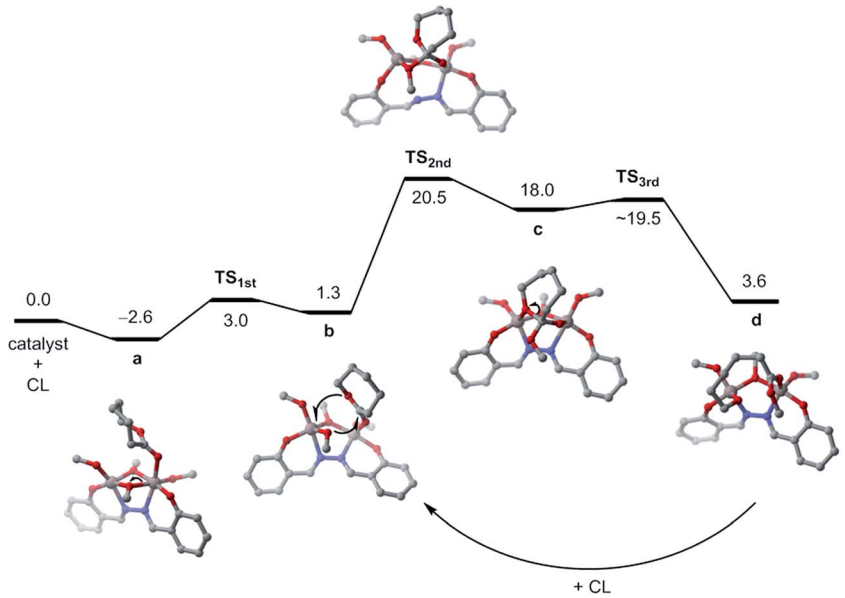

Fig. 10 Possible reaction path for the ring-opening polymerization of ε-caprolactone catalyzed by a dinuclear Al catalyst; the relative free energies are shown in kcal mol^{-1} and the geometries of TS_{1st} and TS_{3rd} respectively resemble those of **b** and **c** and are therefore not shown.

mechanism study using DFT calculations revealed that the cooperation that coordinated the CL with one Al center was initiated by the benzyl alkoxide of another Al center.

4. Experimental section

Standard Schlenk techniques and a N_2-filled glovebox were used all over the isolation and treatment of all the compounds. Solvents, ε-caprolactone, and deuterated solvents were purified prior to use. Salicylaldehyde, 3,5-di-*tert*-butyl-2-hydroxybenzaldehyde, 4-chlorobenzaldehyde, hydrazine monohydrate, ethane-1,2-diamine, benzyl amine, and benzyl alcohol were purchased from Aldrich. ^{1}H and ^{13}C NMR spectra were recorded on a Varian Gemini2000-200 (200 MHz for ^{1}H and 50 MHz for ^{13}C) spectrometer with chemical shifts given in ppm from the internal TMS or center line of $CDCl_3$. Microanalyses were performed using a Heraeus CHN-O-RAPID instrument. The gel permeation chromatography (GPC) measurements were performed on a Waters 1515 Isotratic HPLC pump system equipped with a differential Waters 2414 refractive index detector using THF (HPLC grade) as the eluent. The chromatographic column was a Water Styragel Column (HR4E), and the calibration curve was made by polystyrene standards to calculate M_n(GPC). Ligands of L^{N2Bu}-H,[7] L^{N-NH}-H,[9a] L^{N-NBu}-H,[9b] L^{ClH}-H,[7a] L^{HBu}-H,[9c] L^{Bu}-H,[9d] L^{Bn}-H,[11] and Al complexes of L^{HBu}-$AlMe_2$ (**6**) (ref. 3*d* and 4*r*) and L^{Bu}-$AlMe_2$ (**7**) (ref. 10) were prepared following literature procedures. All the symmetrical ligands were reacted with two equivalent of $AlMe_3$ in toluene to obtain a moderate yield of Al compounds (Scheme 1(A) and (B)). The synthesis of L^{HBu}-$AlMe_2$ (**6**), L^{Bu}-$AlMe_2$ (**7**), L^{HBn}-$AlMe_2$ (**8**), L^{ClH}-$AlMe_2$ (**4**), and L^{ClBu}-$AlMe_2$ (**5**) was similar to the aforementioned method except that one equivalent of $AlMe_3$ was used. DFT geometry optimizations were carried out at M06/6-31G* level combined with the D3 version of Grimme's dispersion correction. Calculations were performed by Gaussian 09 program.

4.1. Synthesis of L^{ClBu}-H

4-Chlorobenzaldehyde (7.03 g, 50 mmol) was added drop-wise into an ethanol solution (100 mL) of the hydrazine monohydrate (5.0 g, 0.10 mol) at 0 °C for 6 h. Volatile materials were removed under vacuum to give a white powder. 3.685 g of the white powder was reacted with 3,5-di-*tert*-butyl-2-hydroxybenzaldehyde (5.85 g, 25 mmol) in ethanol (100 mL) and refluxed for one day. The product precipitated as a yellow solid which was filtered. Yield: 6.05 g (65%). ^{1}H NMR ($CDCl_3$, 200 MHz): δ 8.77, 8.61 (2H, s, C*H*=N), 7.80, 7.43 (4H, d, $J = 8$ Hz, Ar*H*), 7.46, 7.17 (2H, s, Ar*H*), 7.05–6.92 (2H, m, Ar*H*). ^{13}C NMR ($CDCl_3$, 50 MHz): δ 166.68, 165.24 (*C*=N), 160.23, 157.03, 141.10, 136.80, 132.26, 132.33, 129.69, 128.12, 126.97, 116.79 (Ar), 35.10, 34.15 ($C(CH_3)_3$), 31.45, 29.44 ($C(CH_3)_3$). Mp = 155 °C.

4.2. Synthesis of L^{N2Bu}-Al_2Me_4

A mixture of L^{N2Bu}-H (2.32 g, 5 mmol) and $AlMe_3$ (6 mL, 2.0 M in toluene, 12 mmol) in toluene (25 mL), was stirred at 0 °C for one day. Volatile materials were removed under vacuum to give red mud and then it was washed with hexane (50 mL). The product precipitated as a deep yellow powder which was filtered. Yield: 2.45 g (80%). ^{1}H NMR ($CDCl_3$, 200 MHz): δ 8.57 (2H, s, C*H*=N), 7.62 (2H, s, Ar-*H*), 6.95 (2H, s, Ar-*H*), 1.42, 1.31 (36H, s, $C(CH_3)_3$), −0.60 (12H, s, $Al(CH_3)_2$). ^{13}C NMR ($CDCl_3$, 50 MHz): δ 167.52 (*C*=N), 162.30, 140.85, 140.45, 134.26, 128.81, 116.18 (Ar), 35.30, 34.11 ($C(CH_3)_3$), 31.18, 29.28 ($C(CH_3)_3$), −8.79 ($Al(CH_3)_2$). Anal. calcd (found) for $C_{34}H_{54}N_2O_2Al_2$: C, 70.80 (71.14); H, 9.44 (9.74); N, 4.86 (4.76)%. Mp = 224 °C.

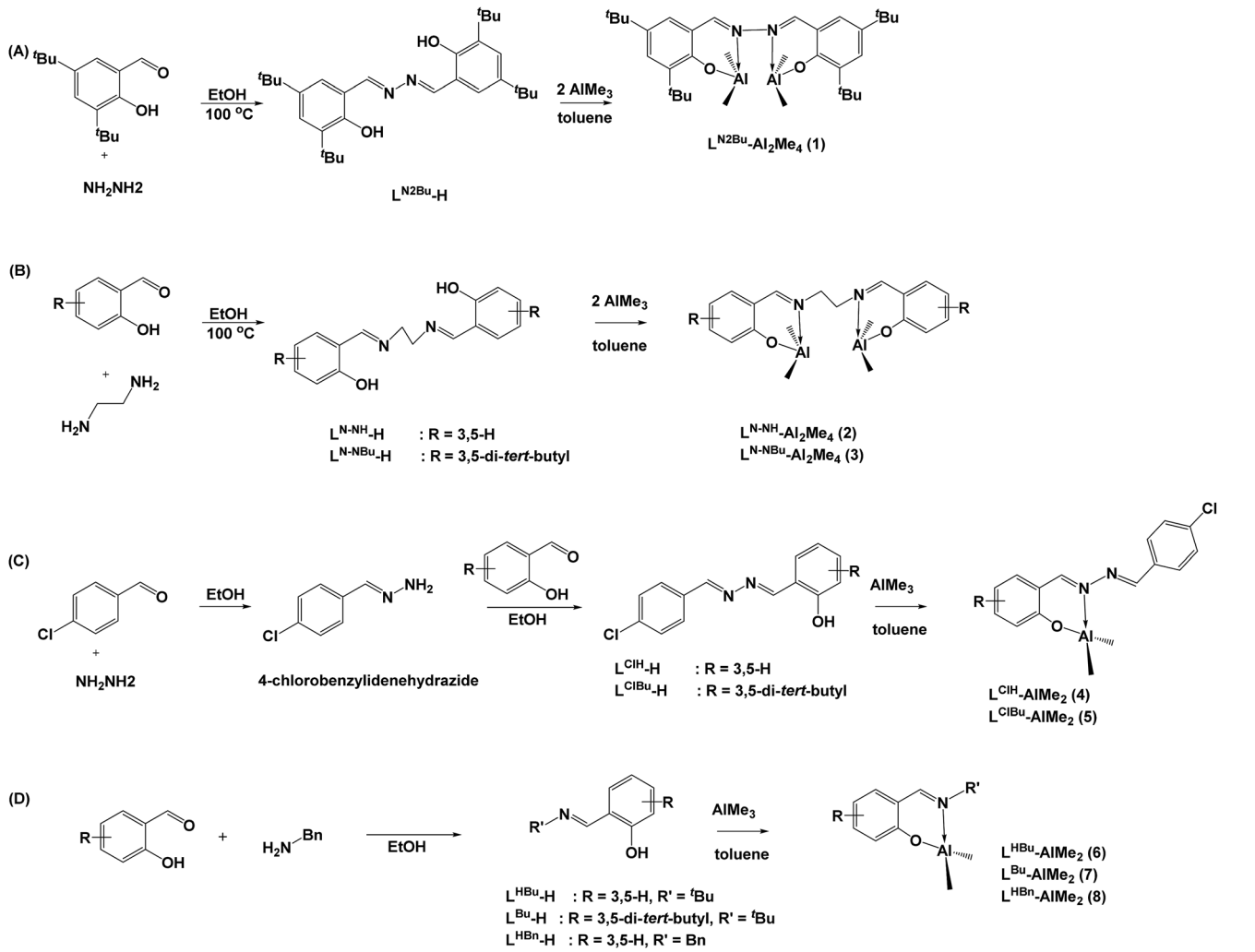

Scheme 1 Synthesis of hydrazine-bridging Schiff base ligands, salen ligands, and associated Al complexes.

4.3. Synthesis of L^{N-NH}-Al_2Me_4

Using a method similar to that for L^{N2Bu}-Al_2Me_4 expect L^{N-NH}-**H** was used in place of L^{N2Bu}-**H**. Yield: 0.99 g (52%). ^{1}H NMR ($CDCl_3$, 200 MHz): δ 8.01 (2H, s, C*H*═N), 7.42 (2H, t, J = 8.0 Hz, Ar-*H*), 7.04 (2H, d, J = 8.0 Hz, Ar-*H*), 6.89 (2H, d, J = 8.0 Hz, Ar-*H*), 6.71 (2H, t, J = 8.0 Hz, Ar-*H*), 3.93 (4H, s, NCH_2CH_2N), −0.67 (12H, s, Al(CH_3)$_2$). ^{13}C NMR ($CDCl_3$, 50 MHz): δ 173.25 (*C*═N), 168.47, 164.08, 137.55, 134.84, 121.59, 117.82 (Ar), 56.21 (NCH_2CH_2N), −9.31 (Al(CH_3)$_2$). Anal. calcd (found) for $C_{20}H_{26}N_2O_2Al_2$: C, 63.15 (63.75); H, 6.89 (6.71); N, 7.36 (7.55)%. Mp = 153 °C.

4.4. Synthesis of L^{N-NBu}-Al_2Me_4

Using a method similar to that for L^{N2Bu}-Al_2Me_4 expect L^{N-NBu}-**H** was used in place of L^{N2Bu}-**H**. Yield: 0.37 g (12%). ^{1}H NMR ($CDCl_3$, 200 MHz): δ 8.01 (2H, s, C*H*═N), 7.50, 6.86 (2H, s, Ar-*H*), 3.87 (4H, s, NCH_2CH_2N), 1.39, 1.22 (36H, s, C(CH_3)$_3$), −0.69 (12H, s, Al(CH_3)$_2$). ^{13}C NMR ($CDCl_3$, 50 MHz): δ 174.23 (*C*═N), 161.73, 140.32, 139.20, 132.54, 128.83, 117.86 (Ar), 56.61 (NCH_2CH_2N), 35.22, 33.93 (*C*(CH$_3$)$_3$), 31.24, 29.27 (C(CH_3)$_3$), −9.18 (Al(CH_3)$_2$). Anal. calcd (found) for $C_{36}H_{58}N_2O_2Al_2$: C, 71.49 (71.82); H, 9.67 (9.56); N, 4.63 (4.99)%. Mp = 180 °C.

4.5. Synthesis of L^{ClH}-$AlMe_2$

A mixture of L^{Cl-H}-**H** (1.29 g, 5 mmol) and $AlMe_3$ (3 mL, 2.0 M in toluene, 6 mmol) in toluene (25 mL), was stirred at 0 °C for one day. Volatile materials were removed under vacuum to give red viscous mud and then it was washed with hexane (50 mL). The product precipitated as a yellow powder which was filtered. Yield: 0.13 g (8%). ^{1}H NMR ($CDCl_3$, 200 MHz): δ 8.72, 8.68 (2H, s, C*H*═N), 7.74, 7.49 (2H, d, J = 8.0 Hz, Ar-*H*), 7.29, 7.28 (2H, m, Ar-*H*), 6.94, 6.84 (2H, m, Ar-*H*), −0.62 (6H, s, Al(CH_3)$_2$). ^{13}C NMR ($CDCl_3$, 50 MHz): δ 169.45, 164.49 (*C*═N), 158.36, 138.49, 137.91, 135.14, 131.09, 129.79, 129.38, 121.61, 118.20, 117.19 (Ar), −9.98 (Al(CH_3)$_2$). Anal. calcd (found) for $C_{16}H_{16}N_2O_2ClAl_2$: C, 61.06 (60.55); H, 5.12 (5.44); N, 8.90 (8.45)%. Mp = 120 °C.

4.6. Synthesis of L^{ClBu}-$AlMe_2$

Using a method similar to that for L^{ClH}-$AlMe_2$ expect L^{ClBu}-**H** was used in place of L^{ClH}-**H**. Yield: 1.59 g (74%). ^{1}H NMR

($CDCl_3$, 200 MHz): δ 8.69 (2H, s, C*H*=N), 7.72, 7.47 (4H, d, J = 8.0 Hz, Ar-*H*), 7.59, 7.10 (2H, s, Ar-*H*), 1.42, 1.31 (18H, s, $C(CH_3)_3$), −0.63 (6H, s, $Al(CH_3)_2$). ^{13}C NMR ($CDCl_3$, 50 MHz): δ 170.57, 162.13 (*C*=N), 157.24, 140.34, 139.74, 138.12, 133.10, 131.38, 129.62, 128.99, 116.76 (Ar), 35.25, 34.07 ($C(CH_3)_3$), 31.27, 29.30 ($C(CH_3)_3$), −8.83 ($Al(CH_3)_2$). Anal. calcd (found) for $C_{24}H_{32}N_2OClAl$: C, 67.51 (67.75); H, 7.55 (7.47); N, 6.56 (6.66)%. Mp = 150 °C.

4.7. Synthesis of L^{Bn}-$AlMe_2$

Using a method similar to that for L^{ClH}-$AlMe_2$ expect L^{Bn}-**H** was used in place of L^{ClH}-**H**. Yield: 1.09 g (82%). ^{1}H NMR ($CDCl_3$, 200 MHz): δ 7.88 (1H, s, C*H*=N), 7.35 (5H, br, Bn-*H*) 7.17–6.95, 6.66–6.57 (4H, m, Ar-*H*), 5.15, 4.80 (2H, d, J = 14 Hz, CH_2Ph), −0.85 (6H, s, $Al(CH_3)_2$). ^{13}C NMR ($CDCl_3$, 50 MHz): δ 167.36 (*C*=N), 163.89, 137.56, 134.28, 133.08, 129.26, 128.67, 128.15, 119.80, 116.65, 114.61 (Ar), 58.65 (CH_2Ph), −7.74 ($Al(CH_3)_2$). Anal. calcd (found) for $C_{16}H_{18}NOAl$: C, 71.89 (71.48); H, 6.79 (7.01); N, 5.24 (5.33)%. Mp = 125 °C.

4.8. General procedures for the polymerization of PCL

A typical polymerization procedure was exemplified by the synthesis of entry 1 (Table 1) using complex L^{N2Bu}-Al_2Me_4 as a catalyst and BnOH as an initiator. The polymerization conversion was analyzed by ^{1}H NMR spectroscopic studies. Toluene (5.0 mL) was added to a mixture of complex L^{N2Bu}-Al_2Me_4 (0.058 g, 0.1 mmol) and CL (1.14 g, 10 mmol) at room temperature. After the solution was stirred for 90 min, the reaction was then quenched by adding to a drop of ethanol, and the polymer was precipitated pouring into *n*-hexane (80.0 mL) to give white solids. The white solid was dissolved in CH_2Cl_2 (5.0 mL) and then *n*-hexane (70.0 mL) was added to give white crystalline solid. Yield: 1.09 g (95%).

4.9. Computational methods

The B3LYP functional[12] was adopted in the present DFT calculations. To remedy the inaccurate treatment of the B3LYP method in dispersion force, the D3 version of dispersion correction developed by Grimme's group was added.[13] Geometry optimizations were carried out in the gas phase at B3LYP-D3/6-31+G(d) level. The nature of the obtained stationary points was confirmed by vibrational frequency analyses at the same level of theory. To obtain more accurate energies, single point energy calculations employing a larger basis set 6-311+G(d,p) were performed and the solvent effects of toluene treated by the SMD continuum solvation model[14] were included. Pure d basis functions (*i.e.*, 5 d functions) were used in the present calculations. Thermal corrections to Gibbs free energy were done at the standard conditions of 298.15 K and 1 atm. Connections between transition states and their corresponding intermediates were justified by geometry optimizations with initial structures derived from displacing the geometries of transition states a little bit along the imaginary vibrational vector. All calculations were accomplished by the Gaussian 09 program.[15]

We would like to mention that our endeavors to locate the transition state $\mathbf{TS_{3rd}}$ for the ring-opening step (**c** → **d**) failed. Instead, we performed the calculation of potential energy surface scan from **c** to **d** with increasing the $C_{carbonyl}$–O_{ester} bond length and approximately identified the maximum point along the scan path as the $\mathbf{TS_{3rd}}$. Vibrational frequency analysis of this approximate $\mathbf{TS_{3rd}}$ indeed shows an imaginary vibration corresponding to the $C_{carbonyl}$–O_{ester} bond stretching.

Acknowledgements

This study is supported by Kaohsiung Medical University "Aim for the top 500 universities grant" under Grant No. KMU-DT105009, NSYSU-KMU JOINT RESEARCH PROJECT, (#NSYSUKMU 105-I004), and the Ministry of Science and Technology (Grant MOST 105-2113-M-037-007). We thank Center for Research Resources and Development at Kaohsiung Medical University for the instrumentation and equipment support.

References

1 (*a*) W. Mattanavee, O. Suwantong, S. Puthong, T. Bunaprasert, V. P. Hoven and P. Supaphol, *ACS Appl. Mater. Interfaces*, 2009, **1**, 1076–1085; (*b*) N. E. Zander, J. A. Orlicki, A. M. Rawlett and T. P. Beebe Jr, *ACS Appl. Mater. Interfaces*, 2012, **4**, 2074–2081; (*c*) S. Tarafder and S. Bose, *ACS Appl. Mater. Interfaces*, 2014, **6**, 9955–9965; (*d*) O. Castaño, N. Sachot, E. Xuriguera, E. Engel, J. A. Planell, J.-H. Park, G.-Z. Jin, T.-H. Kim, J.-H. Kim and H.-W. Kim, *ACS Appl. Mater. Interfaces*, 2014, **6**, 7512–7522; (*e*) E. A. Rainbolt, K. E. Washington, M. C. Biewer and M. C. Stefan, *Polym. Chem.*, 2015, **6**, 2369–2381; (*f*) L. C. Palmer, C. J. Newcomb, S. R. Kaltz, E. D. Spoerke and S. I. Stupp, *Chem. Rev.*, 2008, **108**, 4754–4783; (*g*) D. J. A. Cameron and M. P. Shaver, *Chem. Soc. Rev.*, 2011, **40**, 1761–1776; (*h*) J. Nicolas, S. Mura, D. Brambilla, N. Mackiewicz and P. Couvreur, *Chem. Soc. Rev.*, 2013, **42**, 1147–1235; (*i*) C. G. Palivan, R. Goers, A. Najer, X. Zhang, A. Car and W. Meier, *Chem. Soc. Rev.*, 2016, **45**, 377–411.

2 (*a*) C. A. Wheaton, P. G. Hayes and B. J. Ireland, *Dalton Trans.*, 2009, 4832–4846; (*b*) S. M. Guillaume, E. Kirillov, Y. Sarazin and J.-F. Carpentier, *Chem.–Eur. J.*, 2015, **21**, 7988–8003; (*c*) J.-F. Carpentier, *Organometallics*, 2015, **34**, 4175–4189; (*d*) S. Bellemin and S. Dagorne, *Chem. Rev.*, 2014, **114**, 8747–8774; (*e*) E. Piedra-Arroni, A. Amgoune and D. Bourissou, *Dalton Trans.*, 2013, **42**, 9024–9029; (*f*) N. Ajellal, J.-F. Carpentier, C. Guillaume, S. M. Guillaume, M. Helou, V. Poirier, Y. Sarazin and A. Trifonov, *Dalton Trans.*, 2010, **39**, 8363–8376; (*g*) J. N. Hoskins and S. M. Grayson, *Polym. Chem.*, 2011, **2**, 289–299; (*h*) C. M. Thomas, *Chem. Soc. Rev.*, 2010, **39**, 165–173; (*i*) A. Arbaoui and C. Redshaw, *Polym. Chem.*, 2010, **1**, 801–826.

3 (*a*) J. Lewiński, P. Horeglad, M. Dranka and I. Justyniak, *Inorg. Chem.*, 2004, **43**, 5789–5791; (*b*) N. Nomura, T. Aoyama, R. Ishii and T. Kondo, *Macromolecules*, 2005, **38**, 5363–5366; (*c*) N. Iwasa, J. Liu and K. Nomura, *Catal. Commun.*, 2008, **9**, 1148–1152; (*d*) J. Liu, N. Iwasa and K. Nomura, *Dalton Trans.*, 2008, 3978–3988; (*e*) N. Iwasa, M. Fujiki and K. Nomura, *J. Mol. Catal. A: Chem.*, 2008,

292, 67–75; (*f*) N. Iwasa, S. Katao, J. Liu, M. Fujiki, Y. Furukawa and K. Nomura, *Organometallics*, 2009, **28**, 2179–2187; (*g*) J. Wu, X. Pan, N. Tang and C.-C. Lin, *Eur. Polym. J.*, 2007, **43**, 5040–5046; (*h*) Z.-X. Du, J.-T. Xu, Y. Yang and Z.-Q. Fan, *J. Appl. Polym. Sci.*, 2007, **105**, 771–776; (*i*) C. Zhang and Z.-X. Wang, *J. Organomet. Chem.*, 2008, **693**, 3151–3158; (*j*) K. V. Zaitsev, Y. A. Piskun, Y. F. Oprunenko, S. S. Karlov, G. S. Zaitseva, I. V. Vasilenko, A. V. Churakov and S. V. Kostjuk, *J. Polym. Sci., Part A: Polym. Chem.*, 2014, **52**, 1237–1250; (*k*) A. Gao, Y. Mu, J. Zhang and W. Yao, *Eur. J. Inorg. Chem.*, 2009, 3613–3621; (*l*) D. Pappalardo, L. Annunziata and C. Pellecchia, *Macromolecules*, 2009, **42**, 6056–6062; (*m*) S. Tabthong, T. Nanok, P. Kongsaeree, S. Prabpaib and P. Hormnirun, *Dalton Trans.*, 2014, **43**, 1348–1359; (*n*) M. Shen, W. Zhang, K. Nomura and W.-H. Sun, *Dalton Trans.*, 2009, 9000–9009; (*o*) W. Zhang, Y. Wang, W.-H. Sun, L. Wang and C. Redshaw, *Dalton Trans.*, 2012, **41**, 11587–11596; (*p*) K. Matsubara, C. Terata, H. Sekine, K. Yamatani, T. Harada, K. Eda, M. Dan, Y. Koga and M. Yasuniwa, *J. Polym. Sci., Part A: Polym. Chem.*, 2012, **50**, 957–966; (*q*) I. V. D. Meulen, E. Gubbels, S. Huijser, R. Sablong, C. E. Koning, A. Heise and R. Duchateau, *Macromolecules*, 2011, **44**, 4301–4305; (*r*) A. Meduri, T. Fuoco, M. Lamberti, C. Pellecchia and D. Pappalardo, *Macromolecules*, 2014, **47**, 534–543.

4 (*a*) L. M. Alcazar-Roman, B. J. O'Keefe, M. A. Hillmyer and W. B. Tolman, *Dalton Trans.*, 2003, 3082–3087; (*b*) Z. Tang and V. C. Gibson, *Eur. Polym. J.*, 2007, **43**, 150–155; (*c*) K. Ding, M. O. Miranda, B. Moscato-Goodpaster, N. Ajellal, L. E. Breyfogle, E. D. Hermes, C. P. Schaller, S. E. Roe, C. J. Cramer, M. A. Hillmyer and W. B. Tolman, *Macromolecules*, 2012, **45**, 5387–5396; (*d*) H. Du, A. H. Velders, P. J. Dijkstra, J. Sun, Z. Zhong, X. Chen and J. Feijen, *Chem.–Eur. J.*, 2009, **15**, 9836–9845; (*e*) R.-C. Yu, C.-H. Hung, J.-H. Huang, H.-Y. Lee and J.-T. Chen, *Inorg. Chem.*, 2002, **41**, 6450–6455; (*f*) H.-C. Tseng, M. Y. Chiang, W.-Y. Lu, Y.-J. Chen, C.-J. Lian, Y.-H. Chen, H.-Y. Tsai, Y.-C. Lai and H.-Y. Chen, *Dalton Trans.*, 2015, **44**, 11763–11773; (*g*) D. J. Darensbourg, P. Ganguly and D. Billodeaux, *Macromolecules*, 2005, **38**, 5406–5410; (*h*) A. Bhaw-Luximon, D. Jhurry and N. Spassky, *Polym. Bull.*, 2000, **44**, 31–38; (*i*) P. Hormnirun, E. L. Marshall, V. C. Gibson, A. J. P. White and D. J. Williams, *J. Am. Chem. Soc.*, 2004, **126**, 2688–2689; (*j*) X. Pang, H. Du, X. Chen, X. Wang and X. Jing, *Chem.–Eur. J.*, 2008, **14**, 3126–3136; (*k*) X. Pang, H. Du, X. Chen, X. Zhuang, D. Cui and X. Jing, *J. Polym. Sci., Part A: Polym. Chem.*, 2005, **43**, 6605–6612; (*l*) X. Pang, X. Chen, H. Du, X. Wang and X. Jing, *J. Organomet. Chem.*, 2007, **692**, 5605–5613; (*m*) W.-H. Sun, M. Shen, W. Zhang, W. Huang, S. Liu and C. Redshaw, *Dalton Trans.*, 2011, **40**, 2645–2653; (*n*) C. Bakewell, R. H. Platel, S. K. Cary, S. M. Hubbard, J. M. Roaf, A. C. Levine, A. J. P. White, N. J. Long, M. Haaf and C. K. Williams, *Organometallics*, 2012, **31**, 4729–4736; (*o*) S. Gong and H. Ma, *Dalton Trans.*, 2008, 3345–3357; (*p*) W.-A. Ma, L. Wang and Z.-X. Wang, *Dalton Trans.*, 2011, **40**, 4669–4677; (*q*) H.-C. Tseng, M. Y. Chiang, W.-Y. Lu, Y.-J. Chen, C.-J. Lian, Y.-H. Chen, H.-Y. Tsai, Y.-C. Lai and H.-Y. Chen, *Dalton Trans.*, 2015, **44**, 11763–11773; (*r*) M.-C. Chang, W.-Y. Lu, H.-Y. Chang, Y.-C. Lai, M. Y. Chiang, H.-Y. Chen and H. Y. Chen, *Inorg. Chem.*, 2015, **54**, 11292–11298; (*s*) M. O. Miranda, Y. DePorre, H. Vazquez-Lima, M. A. Johnson, D. J. Marell, C. J. Cramer and W. B. Tolman, *Inorg. Chem.*, 2013, **52**, 13692–13701.

5 (*a*) W. Li, W. Wu, Y. Wang, Y. Yao, Y. Zhang and Q. Shen, *Dalton Trans.*, 2011, **40**, 11378–11381; (*b*) Y. Wang and H. Ma, *Chem. Commun.*, 2012, **48**, 6729–6731; (*c*) X. Pang, R. Duan, X. Li, Z. Sun, H. Zhang, X. Wang and X. Chen, *Polym. Chem.*, 2014, **5**, 6857–6864; (*d*) T. R. Forder and M. D. Jones, *New J. Chem.*, 2015, **39**, 1974–1978; (*e*) D. J. Darensbourg and O. Karroonnirun, *Organometallics*, 2010, **29**, 5627–5634; (*f*) D. J. Darensbourg, O. Karroonnirun and S. J. Wilson, *Inorg. Chem.*, 2011, **50**, 6775–6787; (*g*) J. Yang, Y. Yu, Q. Li, Y. Li and A. Cao, *J. Polym. Sci., Part A: Polym. Chem.*, 2005, **43**, 373–384; (*h*) C. Kan, J. Ge and H. Ma, *Dalton Trans.*, 2016, **45**, 6682–6695; (*i*) Z. Sun, R. Duan, J. Yang, H. Zhang, S. Li, X. Pang, W. Chen and X. Chen, *RSC Adv.*, 2016, **6**, 17531–17538; (*j*) N. Maudoux, T. Roisonel, V. Dorcet, J.-F. Carpentier and Y. Sarazin, *Chem.–Eur. J.*, 2014, **20**, 6131–6147; (*k*) H.-L. Chen, S. Dutta, P.-Y. Huang and C.-C. Lin, *Organometallics*, 2012, **31**, 2016–2025; (*l*) C. Kan and H. Ma, *RSC Adv.*, 2016, **6**, 47402–47409; (*m*) Z. Qu, R. Duan, X. Pang, B. Gao, X. Li, Z. Tang, X. Wang and X. Chen, *J. Polym. Sci., Part A: Polym. Chem.*, 2014, **52**, 1344–1352; (*n*) X. Pang, R. Duan, X. Li and X. Chen, *Polym. Chem.*, 2014, **5**, 3894–3900; (*o*) L. Li, B. Liu, C. Wu, S. Li, B. Liu and D. Cui, *Organometallics*, 2014, **33**, 6474–6480; (*p*) W. Yao, Y. Mu, A. Gao, W. Gao and L. Ye, *Dalton Trans.*, 2008, 3199–3206; (*q*) L. E. N. Allan, J. A. Bélanger, L. M. Callaghan, D. J. A. Cameron, A. Decken and M. P. Shaver, *J. Organomet. Chem.*, 2012, **706–707**, 106–112; (*r*) S. Doherty, R. J. Errington, N. Housley and W. Clegg, *Organometallics*, 2004, **23**, 2382–2388; (*s*) W. Ziemkowska, S. Kucharski, A. Kolodziej and R. Anulewicz-Ostrowska, *J. Organomet. Chem.*, 2004, **689**, 2930–2939; (*t*) W. Ziemkowska, J. Kochanowski and M. K. Cyrański, *J. Organomet. Chem.*, 2010, **695**, 1205–1209.

6 (*a*) L. Chen, W. Li, D. Yuan, Y. Zhang, Q. Shen and Y. Yao, *Inorg. Chem.*, 2015, **54**, 4699–4708; (*b*) X.-F. Yu and Z.-X. Wang, *Dalton Trans.*, 2013, **42**, 3860–3868; (*c*) A. Arbaoui, C. Redshaw and D. L. Hughes, *Chem. Commun.*, 2008, 4717–4719; (*d*) H.-L. Han, Y. Liu, J.-Y. Liu, K. Nomura and Y.-S. Li, *Dalton Trans.*, 2013, **42**, 12346–12353; (*e*) M. Normand, T. Roisonel, J.-F. Carpentier and E. Kirillov, *Chem. Commun.*, 2013, **49**, 11692–11694; (*f*) H.-C. Huang, B. Wang, Y.-P. Zhang and Y.-S. Li, *Polym. Chem.*, 2016, **7**, 5819–5827; (*g*) F. Isnard, M. Lamberti, L. Lettieri, I. D'auria, K. Press, R. Troiano and M. Mazzeo, *Dalton Trans.*, 2016, **45**, 16001–16010.

7 (*a*) H.-C. Tseng, H.-Y. Chen, Y.-T. Huang, W.-T. Lu, Y.-L. Chang, M. Y. Chiang, Y.-C. Lai and H.-Y. Chen, *Inorg. Chem.*, 2016, **55**, 1642–1650; (*b*) L. Wang, Q. Su, Q. Wu, W. Gao and Y. Mu, *C. R. Chim.*, 2012, **15**, 463–470.

8 M. S. Bharara, K. Heflin, S. Tonks, K. L. Strawbridge and A. E. V. Gorden, *Dalton Trans.*, 2008, 2966–2973.

9 (*a*) I. Correia, J. C. Pessoa, M. T. Duarte, M. F. M. da Piedade, T. Jackush, T. Kiss, M. M. C. A. Castro, C. F. G. C. Geraldes and F. Avecilla, *Eur. J. Inorg. Chem.*, 2005, 732–744; (*b*) I. A. Fallis, D. M. Murphy, D. J. Willock, R. J. Tucker, R. D. Farley, R. Jenkins and R. R. Strevens, *J. Am. Chem. Soc.*, 2004, **126**, 15660–15661; (*c*) B. D. Clercq and F. Verpoort, *J. Mol. Catal. A: Chem.*, 2002, **180**, 67–76; (*d*) G. Alesso, M. Sanz, M. E. G. Mosquera and T. Cuenca, *Eur. J. Inorg. Chem.*, 2008, 4638–4649; (*e*) A. Duda, Z. Florjanczyk, A. Hofman, S. Slomkowski and S. Penczek, *Macromolecules*, 1990, **23**, 1640–1646.

10 M. S. Hill, A. R. Hutchison, T. S. Keizer, S. Parkin, M. A. VanAelstyn and D. A. Atwood, *J. Organomet. Chem.*, 2001, **628**, 71–75.

11 J. U. Ahmad, M. Nieger, M. R. Sundberg, M. Leskelä and T. Repo, *J. Mol. Struct.*, 2011, **995**, 9–19.

12 (*a*) C. Lee, W. Yang and R. G. Parr, *Phys. Rev. B: Condens. Matter Mater. Phys.*, 1988, **37**, 785–789; (*b*) A. D. Becke, *J. Chem. Phys.*, 1993, **98**, 5648–5652.

13 S. Grimme, J. Antony, S. Ehrlich and H. Krieg, *J. Chem. Phys.*, 2010, **132**, 154104.

14 A. V. Marenich, C. J. Cramer and D. G. Truhlar, *J. Phys. Chem. B*, 2009, **113**, 6378–6396.

15 M. J. Frisch, G. W. Trucks, H. B. Schlegel, G. E. Scuseria, M. A. Robb, J. R. Cheeseman, G. Scalmani, V. Barone, B. Mennucci and G. A. Petersson, *et al.*, *Gaussian 09, revision D.01*, Gaussian, Inc., Wallingford, CT, 2009.

